An Extended Analysis of Texture Descriptors to Improve the Results of Automatic Breast Tumor Segmentations in Ultrasound Images

Fabian Torres, Zian Fanti, Fernando Arambula, Ping-Lang Yen

Abstract

Texture analysis in ultrasound images has been widely used in the medical field to extract relevant information that may help to differentiate several pathologies from healthy tissue, such as breast cancer. Some texture descriptors have been used to improve the results of breast tumor segmentations in ultrasound images. We present an evaluation of the ability of different texture descriptors to enhance the contrast between breast tumors and healthy tissue in ultrasound images and how they affect the segmentation results. In this work we evaluate descriptors extracted from the analysis of the histogram, co-occurrence and run-length matrices. The contrast between the tumor region and healthy tissue was evaluated using the signal to noise ratio (SNR), contrast to noise ratio (CNR), histogram intersection and Minkowski-form Distance between the tumor region and healthy tissue histograms. We implement a probabilistic segmentation method in order to evaluate the changes in the accuracy, sensitivity, specificity, positive predictive value (PPV) and negative predicted value (NPV) of the method when using different texture descriptors, where the Short Run Emphasis of the run-length matrix had better results with values of 91.02%, 88.58%, 96.89%, 96.34% and 89.16% respectively.

Introduction

Since breast cancer has become the number one cause of death among women around the world, it is important to have accurate diagnostic methods to improve the prognosis of the patient (Jiao & Wang, 2011). Although biopsy is the gold standard for cancer diagnosis, minimal invasion methods for diagnosis are preferred in order to reduce further complications; for this reason, several diagnostic methods using ultrasound images have been proposed. Currently ultrasound is responsible for about one in five of all diagnostic images (Halliwell, 2010), but the visualization of lesions in ultrasound breast images is a difficult task due to some intrinsic characteristics of the images like speckle, acoustic shadows and blurry edges (Chen, Chang, Wu, Moon, & Wu, 2003).

Texture analysis refers to the characterization of regions in an image by their texture content, quantifying intuitive qualities described as roughness, smoothness, silkiness and bumpiness (Rajaei, Dallalzadeh, & Rangarajan, 2012). In ultrasound images echo patterns are generally referred as a kind of texture (Liao, Wu, Li, & Yeh, 2011); a good breast tumor segmentation method in ultrasound images should take into account texture features in order to differentiate tumors from other objects with similar gray intensities like glands and acoustic shadows (Madabhushi & Metaxas, 2003), but texture analysis in ultrasound images is not an easy task and many texture metrics have been used to model the echo patterns in breast tumors. Several automatic and semi-automatic segmentation methods using pixel intensity along with texture information have been proposed (Madabhushi & Metaxas, 2003). Some of these methods use first-order texture descriptors obtained from histogram statistics (S.-F. Huang, Chen, & Woo, 2008; Madabhushi & Metaxas, 2003), but these descriptors are not able to give a good texture description in ultrasound images because they do not take into account the spatial relation

between pixels and gray-levels (Bader et al., 2000); because of this, other proposed methods use second-order texture descriptors extracted from co-occurrence matrices statistics (Liu et al., 2010), but the computational cost for computing the co-occurrence matrix is very high and much more demanding while working in per-pixel computation (F. Igual R. Mayo & M.Ujaldon, 2008). Other texture descriptors extracted from run-length matrices statistics have been used for breast tumor classification in ultrasound images.

Texture is a rich source of visual information and there are a number of methods for texture representation, because of this, it is difficult to define the properties that can be used to effectively distinguish textures found in a given image (Yassine, Belfkih, Najah, & Zenkouar, 2010). For this reason, it is important to evaluate which texture descriptor is the one that improves the outcome of a segmentation method. Here we do an extensive evaluation of how texture descriptors extracted from histogram statistics, co-occurrence matrices statistics and run-length matrices statistics modify the contrast between the tumor region and the surrounding tissue in breast ultrasound images and how this affects the results of an automatic segmentation algorithm, in order to find which are the best texture descriptors to effectively distinguish between healthy tissue and tumors in breast ultrasound images. Except for the work done by Liao *et al.* in (Liao et al., 2011), where they compare the ability of different texture descriptors extracted from co-occurrence matrices statistics to enhance the contrast between the tumor region and the surrounded tissue and how it affects the results of manual segmentation by increasing the visualization of the tumor region in ultrasound images, there is no related work that evaluate the ability of different texture descriptors, extracted from first and second order statistics, to improve the automatic segmentation of tumors in breast ultrasound images. To evaluate the ability of these descriptors to enhance the contrast between the tumor region and the healthy tissue, we obtained a texture image using per-pixel computation using different texture descriptors and compare the signal to noise ratio (SNR), contrast to noise ratio (CNR), histogram intersection and Minkowski-form Distance between the tumor region and healthy tissue histograms in each image. We also evaluate the ability of these descriptors to improve the segmentation results; we implemented a probabilistic segmentation method based on the work of Madabushi *et al.* in (Madabhushi & Metaxas, 2003) and compare the accuracy, sensitivity, specificity, positive predictive value (PPV) and negative predicted value (NPV) of the method when using different texture descriptors.

Texture Analysis

Here we evaluate texture descriptors extracted from histogram statistics, co-occurrence matrices statistics and run-length matrices statistics.

First-order texture descriptors are extracted from the original image values; they do not consider the spatial relationships with neighborhood pixels (Selvarajah & Kodituwakku, 2011). The most frequently used first-order texture descriptors are central moments of the histogram (Aggarwal & Agrawal, 2012). These descriptors have been used for the segmentation and classification of breast tumors in ultrasound images; Huang *et al*. in (S.-F. Huang et al., 2008) use the Mean and Entropy of the histogram to characterize the texture of breast tumors, also the Kurtosis and Skewness of the histogram have been used for tumor classification by Pilouras *et al.* in (Piliouras, Kalatzis, Dimitropoulos, & Cavouras, 2004).

Other descriptors extracted from the image original intensity values have been used; in (Madabhushi & Metaxas, 2003) the difference of the intensity of each pixel with the mean of its neighborhood is used as a texture descriptor.

The gray-level co-occurrence matrix (GLCM) describes how frequently two gray-levels appear in a window separated by a given distance and a given angle (Aggarwal & Agrawal, 2012). Second-order texture descriptors computed from the analysis of the co-occurrence matrices have been proposed in (Haralick, 1979) by Haralick *et al.* Some of these texture descriptors have been used for the segmentation and classification of breast tumors; Liu *et al.* use the entropy and contrast of the co-occurrence matrix for breast tumor segmentation in (Liu et al., 2010). Liao *et al.* evaluate the ability of the homogeneity, contrast, energy and variance of the co-occurrence matrix to enhance the contrast of tumors in breast ultrasound images, concluding that the variance of the co-occurrence matrix is the best texture descriptor of the four to be used in breast tumor contrast enhancement in ultrasound images (Liao et al., 2011). Although these descriptors take into account the spatial relationship between pixels the computational cost of computing the co-occurrence matrix is very high compared to first order descriptors (F. Igual R. Mayo & M.Ujaldon, 2008).

Another method to characterize texture that also takes into account the spatial relationship between pixels is based on run lengths of image gray-levels, where the run-length matrix of an image is defined as the number of runs with pixels of equal gray level and a given run-length (Selvarajah & Kodituwakku, 2011); although these descriptors have not been widely used as an effective texture classification and analysis method, it has been demonstrated by Tang *et al*. in (Tang, 1998) that there is rich texture information contained in this matrices. Galloway *et al.* proposed five texture descriptors based on the analysis of run-length matrices in (Galloway, 1975): short run emphasis (SRE), long run emphasis (LRE), gray-level nonuniformity (GLN), run-length nonuniformity (RLN) and run percentage (RP); these descriptors have been successfully used for the classification of breast tumors in ultrasound images in (Lefebvre, Meunier, Thibault, Laugier, & Berger, 2000; Murmis, Gisvold, Kinter, & Greenleaf, 1988; Piliouras et al., 2004).

Table 1 list the texture descriptors evaluated in this work extracted from histogram, co-occurrence and run-length statistics.

Table 1. List of evaluated texture descriptors.

First order	Mean	(S.-F. Huang et al., 2008)
	Entropy	(S.-F. Huang et al., 2008)
	Kurtosis	(Piliouras et al., 2004)
	Skewness	(Piliouras et al., 2004)
	Mean Difference	(Madabhushi & Metaxas, 2003)
Co-occurrence	Entropy	(Liu et al., 2010)
	Contrast	(Liu et al., 2010)
	Homogeneity	(Liao et al., 2011)
	Energy	(Liao et al., 2011)
	Variance	(Liao et al., 2011)
Run-length	Short Run Emphasis	(Lefebvre et al., 2000)
	Long Run Emphasis	(Lefebvre et al., 2000)
	Gray-Level Nonuniformity	(Murmis et al., 1988)
	Run-length Nonuniformity	(Murmis et al., 1988)

Segmentation Method

Because of inherent artifacts in breast ultrasound images such as speckle and blurry edges, the segmentation of tumors is not an easy task (Chen et al., 2003). Several works have been done in order to create semi-automatic and automatic methods. Based on the literature, these methods can be divided in two groups; thresholding based methods and classifiers based methods. The thresholding based methods have low computational cost and usually used only gray-level intensities of the pixels to segment de image (R.-F. Chang, Wu, Moon, & Chen, 2005; Chen et al., 2003; S.-F. Huang et al., 2008). The classifier based methods are more robust since they use more than one feature for classification, but the implementation and the computational cost increments considerably compared with thresholding based methods (Q.-H. Huang et al., 2012; Jiao & Wang, 2011; Liu et al., 2010; Madabhushi & Metaxas, 2003). The image features used for classifier based methods should be appropriately selected according to the application, texture information might be suitable for ultrasound images (Chen et al., 2003).

In this paper we implemented an automatic segmentation method based on the one proposed in (Madabhushi & Metaxas, 2003). This method is based on a region-growing algorithm applied to a probability image instead of an intensity image. The probability image is constructed with the probabilities of each pixel of belonging to the tumor region, based on the pixel intensity and texture features. Two density probability functions (*pdf*) are constructed using the gray-level intensity and texture features from previously segmented tumors, the joint probability of the two *pdfs* is computed as the pixel probability to belong to a tumor.

Most of the proposed methods for tumor segmentation in breast ultrasound images use a pre-processing step to obtain more homogenous regions and enhance the contrast between the tumor and the surrounding tissue. For contrast enhancement some works used the stick method (R.-F. Chang et al., 2005; Chen et al., 2003; Q.-H. Huang et al., 2012), but Madabushi *et al.* proposed the use of histogram equalization because it is a fast method with good results in tumor enhancement. To obtain more homogenous regions a Gaussian filter was used in (Chen et al., 2003) and a Butterworth filter was used in (Madabhushi & Metaxas, 2003), but Abd *et al.* probe in (Abd-Elmoniem, Youssef, & Kadah, 2002) that the Gaussian Anisotropic Filter has better results in ultrasound images since it preserves boundaries. Based on this, we implement a pre-processing step to obtain a contrast enhanced intensity image using a histogram equalization and then a Gaussian Anisotropic Filter to obtain more homogenous regions while preserving the edges.

To obtain a texture image using the texture descriptors listed in table 1 we use per pixel computation, with the parameters proposed in the different cited works. Because texture parameters characterize the acoustic properties of the tissue (Lefebvre et al., 2000), the texture image was computed from the original image without any pre-processing step to avoid elimination of any texture related information.

After computing the probability image, using the pre-processed intensity and texture joint probability, the method use a region growing algorithm on the probability image to obtain the region that belongs

to the tumor. To include one pixel inside the tumor region it should satisfy two conditions: First, the probability of belonging to the tumor should be inside a range of values between the mean of the tumor region probability by upper and lower thresholds. Second, the immediate neighborhood of the pixel should intersect with the tumor region. The seed point of the region is automatically determined by the method proposed in (Madabhushi & Metaxas, 2003) where you can find the complete description of the method.

Results

A data base of 30 breast ultrasound images with a lesion were acquired with a GE Heatlhcare Voluson 73 in the Changhua Christian Hospital. The images have a size of 181x163 pixels. After manual localization of the breast tumor and the selection of the region of interest the images were inputted to open source software itk-SNAP for image enhancement and semi-automatic segmentation supervised by the specialist.

Contrast enhancement using texture descriptors

Measuring contrast enhancement can be done with different approaches, there is no standardized solution for this, it is important to include several methods for this purpose in order to have a good contrast enhancement evaluation (D.-S. Huang, McGinnity, Heutte, & Zhang, 2010). To evaluate the ability of the texture descriptors listed in table 1 to enhance the contrast between the tumor region and the surrounding tissue we used the signal to noise ratio (SNR) and the contrast to noise ratio (CNR) both used by Liao *et al.* in (Liao et al., 2011).

$$SNR = \frac{\mu_{ROI}}{\sigma_{ROI}}, \tag{1}$$

$$CNR = \frac{|\mu_{ROI} - \mu_{Background}|}{\sigma_{ROI} + \sigma_{Background}}, \tag{2}$$

where μ_{ROI} and $\mu_{Background}$ are mean brightness values of the tumor region (ROI) and the tissue (Background) respectively, and σ_{ROI} and $\sigma_{Background}$ are the standard deviation of the ROI and the background respectively.

In addition to the SNR and CNR we compute the Minkowski-form distance (MD) and the histogram intersection (INT) between the ROI and background regions as similarity measurements between histograms. The Minkowsky distance is often used for computing dissimilarities between histograms (Rubner, Tomasi, & Guibas, n.d.). The intersection of the histograms is a useful similarity measurement between two histograms when the number of pixels between regions is different, it is well suited to deal with scale changes (Barla, Odone, & Verri, n.d.).

$$MD(H_{ROI}, H_{Background}) = \left(\sum_i |H_{ROI}(i) - H_{Background}(i)|\right), \tag{3}$$

$$INT\left(H_{ROI}, H_{Background}\right) = 1 - \frac{\sum_i \min(H_{ROI}(i), H_{Background}(i))}{\sum_i H_{Background}(i)}, \tag{4}$$

where H_{ROI} and $H_{Background}$ are the normalized histograms of the ROI and the background.

Along with contrast enhancement, another important aspect to take into account when using texture analysis for image segmentation is the ability of the descriptor to preserve the edges of the structures we want to segment (Liao et al., 2011). To evaluate this, we used the edge preservation index (EPI) defined as

$$EPI = \frac{\sum |p_T(i,j) - p_T(i-1, j+1)|}{\sum |p_o(i,j) - p_o(i-1, i+1)|}, \tag{5}$$

where $p_T(i,j)$ is the value of the texture image pixel and $p_o(i,j)$ is the value of the original image; $p_T(i,j)$ and $p_o(i,j)$ are in the edge area, previously segmented in the original image (Han Chumning, Guo Huadong, & Wang Changlin, 2002).

We compare the SNR, CNR, DM, INT and EPI of the original images with the texture images obtained using per-pixel computation with the descriptors listed in table 1. The first order descriptor that obtained better results enhancing the image was the Mean of the histogram with higher values of DM, INT and CNR than the original image, however the SNR was lower than in the original image and the ability to preserve borders was low; the SNR and the EPI were improved by the Entropy and Mean Difference descriptors respectively, however the other contrast enhancement indexes had no good results using this descriptors. Except for the Variance and Energy, all the Haralick texture descriptors improved the SNR significantly but the DM, INT, CNR and EPI were reduced considerably using these descriptors; although none of these descriptors improve the contrast of the image, the Homogeneity of the co-occurrence matrix had higher values in all measurements than the other co-occurrence based descriptors. Of all the Run-length texture descriptors the SRE of the run-length matrix have better results improving the DM, INT, SNR and CNR of the image. As the Haralick texture descriptors, none of the run length texture descriptors was able to preserve borders, decreasing the EPI significantly.

Table 2 shows the results of DM, INT, SNR, CNR and EPI for the original image, while table 3 shows which texture descriptors improve each contrast index. The results for the pre-processing stage used in the segmentation algorithm to obtain an intensity image with a higher contrast are also shown in table 3.

Table 2. Original image contrast indexes

MD	INT	SNR	CNR	EPI
1.4136 ±0.3264	0.2932 ±0.1632	1.7450 ±0.5285	1.0784 ±0.3316	1 ±0

Table 3 shows that the mean of the histogram is the first order descriptor that enhance the highest number of contrast indexes (DM, INT and CNR) but the signal to noise ratio and edge preserving index

are lower than in the original image; of all the texture descriptors listed in table 1, the only one that was able to preserve edges was the one proposed by Madabushi *et al.* in (Madabhushi & Metaxas, 2003). The results also show that using second order descriptors based on the co-occurrence matrix for image enhancement is not useful since none of the texture descriptors proposed by Haralick *et al.* in (Haralick, 1979) are able to enhance the contrast of the image, but the SNR of the tumor region was highly increased using the homogeneity and correlation of the co-occurrence matrix; looking at equation 1 a higher SNR value may imply two things, the mean gray-level of the region increased and/or the standard deviation of the region decreased, making the region brighter and/or more homogenous, but if the contrast between the region and the background is diminished the visualization of the region of interest is going to be more difficult, since the mean gray-level and the homogeneity of the regions is very similar, figure 1 shows how a breast tumor with high SNR in an ultrasound image does not imply a better visualization of the lesion, where the original image has a SNR value of 1.4940 and a CNR value of 1.4882 and the texture image, obtained using the correlation of the co-occurrence matrix as texture descriptor, has a SNR value of 3.2322 and a CNR value of 0.0744. Regarding to the results of contrast enhancement using run-length texture features, table 3 shows that the SRE of the run-length matrix enhance all the contrast indexes except for the EPI, this texture feature is also the one that enhance the Minkowski-form distance and the histogram intersection the most, making easier the differentiation between regions using their probabilities, since the normalized histogram can be used as the probability density function of each gray-level to belong to a region (Legg, Rosin, Marshall, & Morgan, 2013). Figure 2 shows a breast tumor ultrasound image, the pre-processed intensity image and texture images obtained by per-pixel computation using the Mean of the histogram, the Homogeneity of the co-occurrence matrix and SRE of the run-length matrix texture descriptors, while figure 3 shows the normalized histograms of the background (red) and the tumor region (blue) of each image in figure 2.
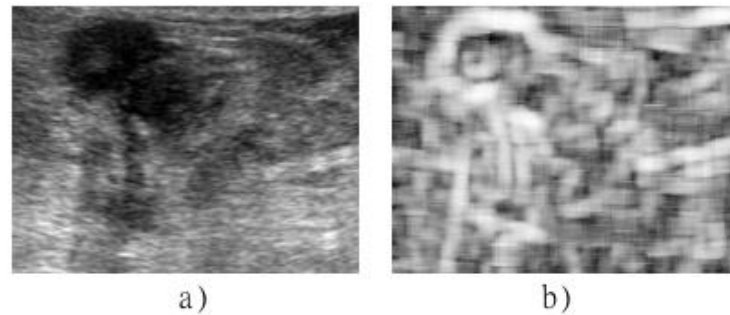

Figure 1. Comparison of lesion visualization with different SNR values a) original image and b) texture image obtained with the correlation of the co-occurrence matrix.

Table 3. Texture descriptors than enhance the contrast

Index	Type		Descriptor	Value
MD	Texture	Histogram	Mean	1.5460 ±0.3075
		Haralick	--	--
		Run-length	LRE	1.4811 ±0.3119
			SRE	1.6217 ±0.2944
	Intensity		Filter	1.4953 ±0.3132
			Filter + Equalization	1.5383 ±0.3067
INT	Texture	Histogram	Mean	0.2270 ±0.1537
		Haralick	--	--
		Run-length	LRE	0.2594 ±0.1559
			SRE	0.1892 ±0.1472
	Intensity		Filter	0.2524 ±0.1566
			Filter + Equalization	0.2308 ±0.1534
SNR	Texture	Histogram	Entropy	3.3629 ±1.0537
			Kurtosis	1.9337 ±0.5872
			Skewness	2.4845 ±0.7100
			Std	2.1388 ±0.5796
		Haralick	Contrast	1.8608 ±0.5232
			Correlation	3.6850 ±0.9207
			Homogeneity	4.0034 ±0.9603
			Variance	1.7103 ±0.3714
		Run-length	GLN	2.6275 ±0.8319
			RLN	2.2124 ±0.4260
			SRE	3.3263 ±1.0729
	Intensity		--	--
CNR	Texture	Histogram	Mean	1.2495 ±0.3713
		Haralick	--	--
		Run-length	SRE	1.2144 ±0.3924
	Intensity		Filter	1.1682 ±0.3610
			Equalization	1.1105 ±0.3408
			Filter + Equalization	1.1682 ±0.3610
EPI	Texture	Histogram	Difference	1.6522 ±0.2802
		Haralick	--	--
		Run-length	--	--
	Intensity		Equalization	1.7296 ±0.2863
			Filter + Equalization	1.4429 ±0.3702

Segmentation evaluation

The applied segmentation method is based on the one proposed in (Madabhushi & Metaxas, 2003) and it consists of a pre-processing step to obtain an intensity image and a texture image in order to build a probability image to segment it with a region growing algorithm. The intensity image is obtained by enhancing the contrast with a histogram equalization and homogenizing regions while preserving edges with a gaussian anisotropic filter, the ability of contrast enhancement and edge preserving of this step was also evaluated by the SNR, CNR, INT, DM and EPI indexes in the previous section. Different texture images were obtained using the texture descriptors listed in table 1. Here we evaluate the results of the segmentation method when using different texture descriptors and compare them with the results without using any texture information. To evaluate the segmentation results we used the accuracy, sensitivity, specificity, positive predictive value (PPV) and the negative predictive value NPV (Liu et al., 2010):

$$Accuracy = \frac{TP + TN}{TP + TN + FP + FN}, \qquad (6)$$

$$Sensitivity = \frac{TP}{TP + FN}, \qquad (7)$$

$$Specificity = \frac{TN}{TN + FP}, \qquad (8)$$

$$PPV = \frac{TP}{TP + FP}, \qquad (9)$$

$$NPV = \frac{TN}{TN + FN}, \qquad (10)$$

where TP, TN, FP and FN are the true positive, true negative, false positive and false negative pixels found in the segmentation process. These indexes were evaluated for the 30 images using a cross-validation technique leaving one out. The accuracy is the ratio of correctly classified pixels (true positives and true negatives) in the entire area of the image (Byrd, Zeng, & Chouikha, 2006). The sensitivity and specificity are often used to complement the evaluation of segmentation algorithms, sensitivity is used for measuring how many pixels in the region of interest are correctly segmented, it does not tell anything about how many pixels in the background would be segmented as tumors (Parikh, Mathai, Parikh, Sekhar, & Thomas, 2008); the specificity measures how many pixels in the background are correctly excluded and does not tell if a tumor pixel would not be correctly segmented (H.-H. Chang, Zhuang, Valentino, & Chu, 2009). The positive and negative predictive values are related with the sensitivity, specificity and the size of the tumor region, the predictive values will change between images if the tumor region covers a different percentage of the whole image, it is important to take this into account since breast tumors size change between patients (Akobeng, 2007). Table 4 shows the segmentation results using only the original image without any pre-processing step and using the intensity image obtained using histogram equalization and a gaussian anisotropic filter. The pre-processing step was able to enhance the segmentation results, making the accuracy, specificity and PPV significantly higher, while the sensitivity and NPV were diminished by 1.24% and 0.54% respectively using the pre-processing, although we could consider these differences insignificant these may lead to unwanted segmentation results.

Table 4. Original and Intensity images segmentation results

Image	Accuracy	Sensitivity	Specificity	PPV	NPV
Original	83.89%	86.51%	86.63%	78.94%	88.84%
Intensity	87.13%	85.26%	90.52%	85.96%	88.30%

We also evaluate the ability of the different texture descriptors listed in table 1 to enhance the segmentation results. Almost all of the first order texture descriptors enhanced the segmentation results expect for the NPV where none of the descriptors were able to enhance it. The first order texture descriptor that leads to better segmentation results was the mean of the histogram, having higher percentage of accuracy, sensitivity, PPV and NPV, with values of 90.58%, 89.36%, 94.08% and 87.08% respectively; the higher value of specificity was obtained using the entropy of the histogram, but the difference between the specificity of the mean and the entropy is only of 0.36% making it insignificant;

the NPV was diminish by 1.22% using the mean of the histogram; the only first order descriptor that diminished the accuracy and specificity of the segmentation method was the Kurtosis of the histogram, diminishing it by 0.55% and 2.17% respectively. The accuracy, sensitivity and NPV segmentation results obtained using the Haralick texture descriptors where similar to the ones using the first order descriptors; the higher values of accuracy (90.60%), sensitivity (88.66%) and NPV (87.24%) were obtained with the homogeneity of the co-occurrence matrix, although this texture descriptor also enhance the specificity and PPV of the segmentation the contrast of the co-occurrence matrix increase these indexes significantly, getting values of 96.71% and 96.16% respectively; none of the Haralick texture descriptors was able to increase the NPV value. The results of the segmentation using run-length texture descriptors lead to better results; the LRE and the SRE were the only texture descriptors of the ones listed in table 1 that were able to increase the NPV value, having the highest value (89.16%) using the SRE of the run-length matrix; the highest values of accuracy, specificity and PPV were also obtained using the SRE of the run-length matrix, while the highest value of sensitivity was obtained with the GLN texture descriptor.
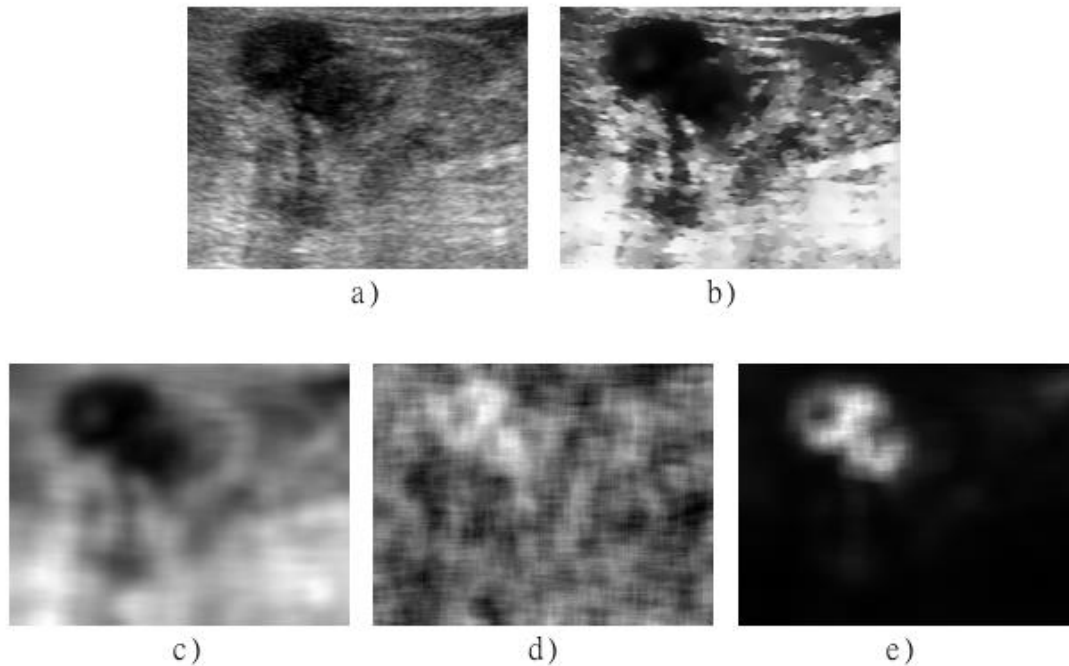

Figure 2. Textural analysis of breast ultrasound images. a) original ultrasound image, b) pre-processed intensity image, c) mean of the histogram texture image, d) Homogeneity of the co-occurrence matrix texture image, and d) SRE of the run-length matrix texture image.

Table 4. Original and Intensity images segmentation results

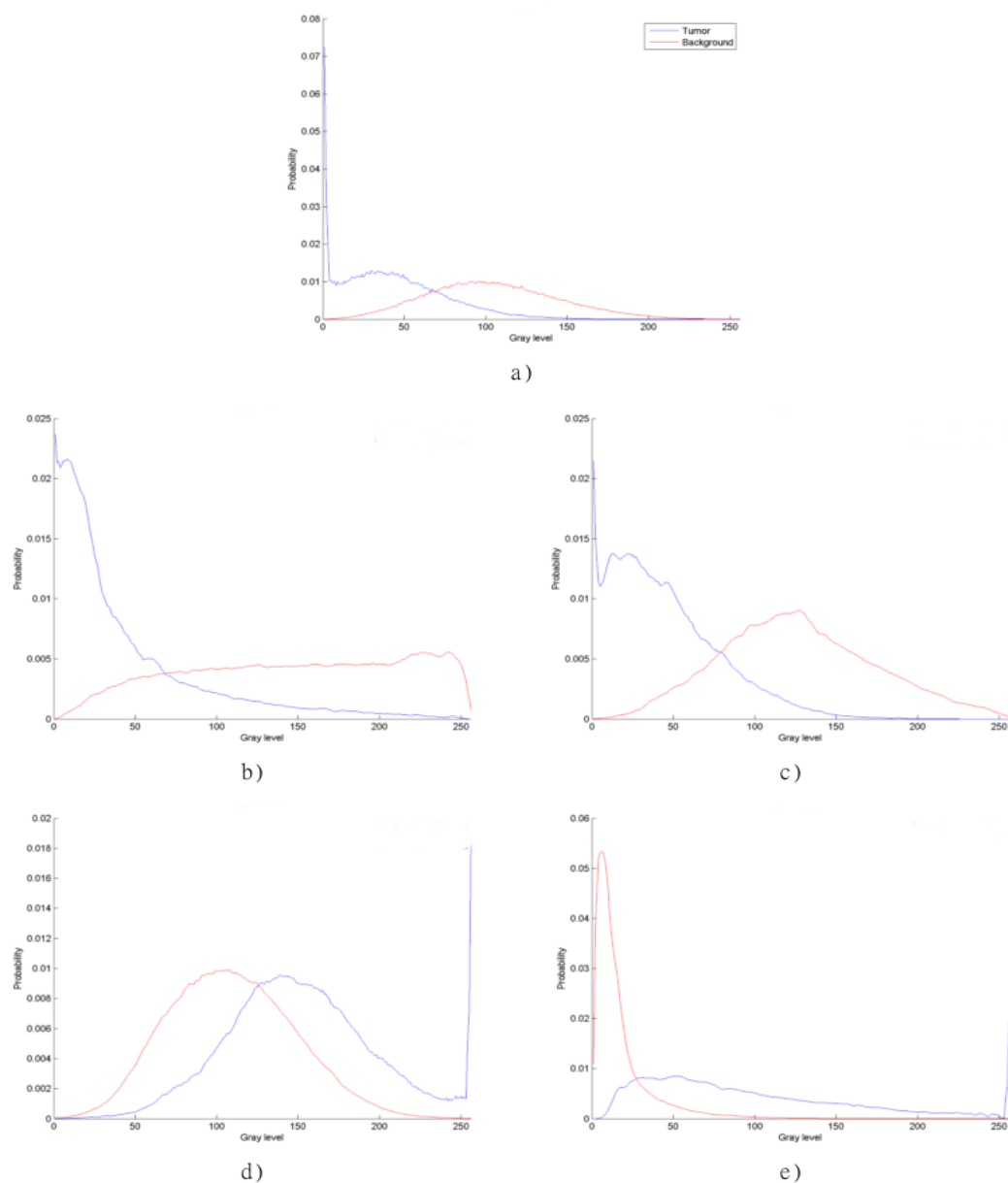| Image	Accuracy	Sensitivity	Specificity	PPV	NPV
Original	83.89%	86.51%	86.63%	78.94%	88.84%
Intensity	87.13%	85.26%	90.52%	85.96%	88.30%

Figure 3. Normalized histograms of textural analysis. a) original ultrasound image, b) pre-processed intensity image, c) mean of the histogram texture image, d) Homogeneity of the co-occurrence matrix texture image, and d) SRE of the run-length matrix texture image.

Table 5. Original and Intensity images segmentation results

Category	Descriptor	Accuracy	Sensitivity	Specificity	PPV	NPV
First Order	Mean	90.58%	89.36%	95.24%	94.08%	87.08%
Haralick	Homogeneity	90.60%	88.66%	94.84%	93.40%	87.24%
Run-length	SRE	91.02%	88.58%	96.89%	96.34%	89.16%

Table 5 shows that using the listed texture descriptors along with the pre-processed image the accuracy, specificity and the PPV can be significantly upgraded, while the increase of sensitivity in the segmentation using texture descriptors is not as significant as in the accuracy, specificity and PPV, it shows that the segmentation results are better than using only the original image or the pre-processed intensity image. While none of the first order and Haralick texture descriptors were able to increase the NPV value of the segmentation, table 5 shows that the SRE was able to increase it by only .32%; although this increment is insignificant, at least this descriptor do not diminish the NPV of the segmentation.

Figure 4 shows the segmentation of a breast tumor in an ultrasound image using different texture descriptors along with the pre-processed intensity image with the probabilistic segmentation method implemented here, it also shows the segmentation results obtained when using only the original intensities of the image and the pre-processed intensity image without any texture information. Table 6 shows the accuracy, sensitivity, specificity, PPV and NPV of the segmented images shown in figure 4.

Table 6. Segmentation results for the segmented images shown in figure 5.

Descriptor	Accuracy	Sensitivity	Specificity	PPV	NPV
Original	82.41%	99.75%	74.03%	64.98%	99.03%
Intensity	91.10%	99.49%	85.14%	82.62%	99.57%
Mean	97.96%	98.50%	97.42%	97.39%	98.52%
Homogeneity	95.97%	98.92%	93.96%	92.96%	98.98%
LRE	98.28%	98.74%	98.84%	98.85%	98.72%

It can be seen in table 6 that using texture descriptors along with a pre-processed intensity image for breast tumor segmentation in the ultrasound image shown in figure 1a) can upgrade the results considerably. Although the sensitivity and NPV are diminished using the texture descriptors, the difference is insignificant (1% and .3% respectively) comparing it with the increase in accuracy, specificity and PPV values (16%, 24% and 34% respectively) using the SRE of the run-length matrix as texture descriptor.
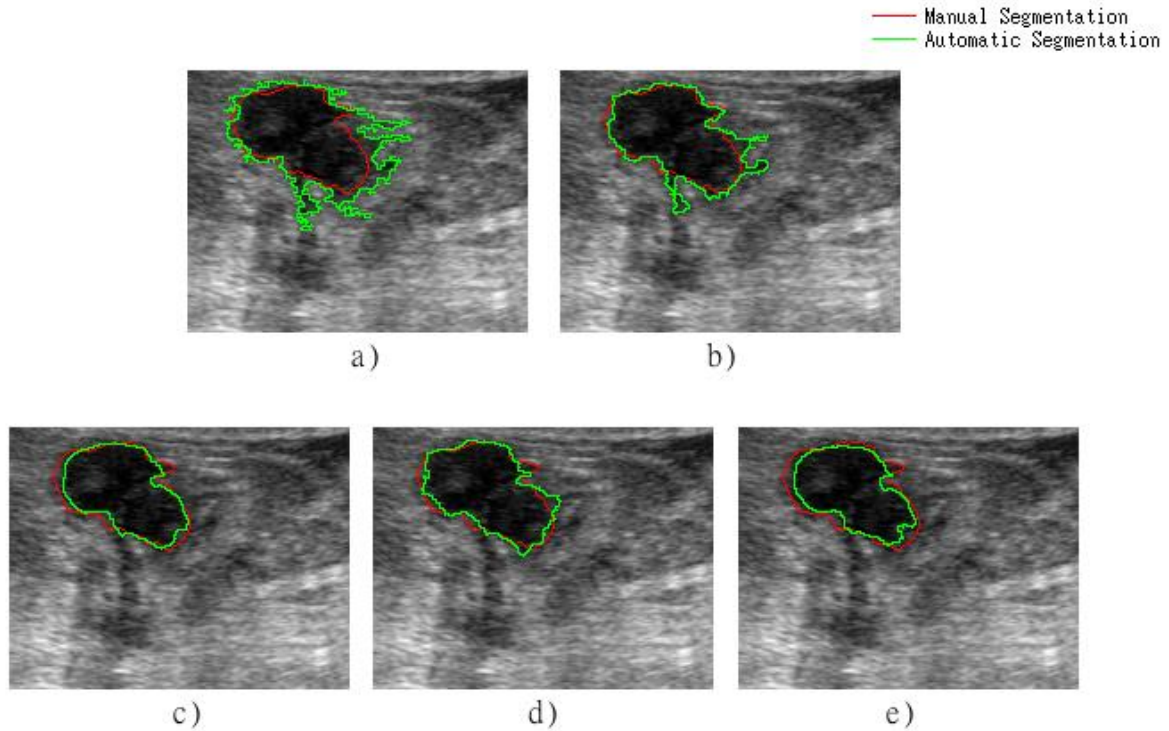
Figure 4. Segmentation of a breast tumor using a) original intensities, b) pre-processed intensity image c) mean of the histogram, c) homogeneity of the co-occurrence matrix, and d) LRE of the run-length matrix.

Discussion and Conclusion

Texture descriptors have been widely used in breast ultrasound images for tumor segmentation, since they help to differentiate structures with similar gray-level intensities as tumors, like acoustic shadows (Madabhushi & Metaxas, 2003). Here we evaluate different texture descriptors in order to find out which one is the most effective to enhance the contrast of the image and which one leads to better segmentation results.

Image quality is a key aspect to consider in ultrasound images since they are affected by many types of artifacts, making it hard for an observer to interpret the images and obtain quantitative and qualitative information from them (Contreras Ortiz, Chiu, & Fox, 2012). Because of the noisy nature of the ultrasound images and the low contrast between breast cancer and surrounding tissue, it is difficult to provide an accurate and effective diagnosis (Guo et al., 2006). The ability of different texture descriptors to enhance the contrast between the tumor region and healthy tissue was evaluated with five indexes (DM, INT, SNR, CNR and EPI). It was shown in the results that some of the texture descriptors listed in table 1 are able to increase one or more of the used contrast indexes, and that SRE of the run-length matrix was able to increase all the indexes but not the EPI; in fact none of the used texture descriptors, except for the difference of the histogram proposed in (Madabhushi & Metaxas, 2003), was able to preserve edges; this may be a drawback when dealing with boundary detection. It was also shown that the co-occurrence based texture descriptors proposed by Haralick *et al.* in (Haralick, 1979) are no good

for image enhancement since none of them was able to increase the value of the contrast indexes, except for the SNR but this may not lead to a better visualization of the tumor region as can be seen in figure 1. The mean of the histogram also showed good results enhancing the contrast of the image, enhancing almost all of the contrast indexes except for the SNR and EPI; this texture descriptor may be used instead of the SRE of the run-length matrix for image enhancement when time is an important factor since first order texture descriptors have lower computational cost than higher order descriptors (Piliouras et al., 2004). The proposed pre-processing intensity step, using histogram equalization and Gaussian anisotropic filtering, showed similar results to the mean of the histogram, but this pre-processing step was able to preserve the edges of the tumor, meaning that it is a good alternative for breast tumor contrast enhancement in ultrasound images.

The results show that although not all of the used texture descriptors enhance the contrast between the tumor region and the healthy tissue, almost all of them enhance the segmentation results of a probabilistic segmentation method like the one implemented here, meaning that texture features provide useful information that helps to distinguish between tumors and healthy tissue in breast ultrasound images. The segmentation was evaluated using five indexes (accuracy, sensitivity, specificity, PPV and NPV), and we use a semi-automatic segmentation supervised by a physician as the gold standard. Table 5 shows that SRE of the run-length matrix is the texture descriptor, of all listed in table 1, that enhance the segmentation results the best, having a significant increase in all of the indexes used here to evaluate the segmentation, except for the NPV where the increase was not significant but the value was not diminished; it is worthy to mention that this texture descriptor is also the one that shows better results in contrast enhancement increasing the MD and decreasing the histogram intersection significantly making easier to differentiate between regions when using the normalized histogram as a probability function. Similar results were obtained using the mean of the histogram and the homogeneity of the co-occurrence matrix, but these two texture descriptors diminished the value of the NPV, although we can consider the difference insignificant.

Here we demonstrate that the use of different texture descriptors give different results in the enhancement and segmentation of breast ultrasound images, some of these descriptors may lead to a better visualization and segmentation of tumors. The results shown that run-length texture descriptors lead to the best results, but other texture descriptors may be used with good results. It may be worthy in future work to evaluate the segmentation results when using more than one texture descriptor and which is the best combination to increase the segmentation results.

References

Abd-Elmoniem, K. Z., Youssef, A.-B. M., & Kadah, Y. M. (2002). Real-time speckle reduction and coherence enhancement in ultrasound imaging via nonlinear anisotropic diffusion. *IEEE Transactions on Biomedical Engineering*, *49*(9), 997–1014. Retrieved from http://www.scopus.com/inward/record.url?eid=2-s2.0-0036721081&partnerID=40&md5=d5f5fbf546ad5e4399367f427a718bd0

Aggarwal, N., & Agrawal, R. K. (2012). First and Second Order Statistics Features for Classification of Magnetic Resonance Brain Images. *Journal of Signal and Information Processing*, *3*(May), 146–153.

Akobeng, A. K. (2007). Understanding diagnostic tests 1: sensitivity, specificity and predictive values. *Acta Paediatrica (Oslo, Norway : 1992)*, *96*(3), 338–41. doi:10.1111/j.1651-2227.2006.00180.x

Bader, W., Böhmer, S., Van Leeuwen, P., Hackmann, J., Westhof, G., & Hatzmann, W. (2000). Does texture analysis improve breast ultrasound precision? *Ultrasound in Obstetrics and Gynecology*, *15*(4), 311–316. Retrieved from http://www.scopus.com/inward/record.url?eid=2-s2.0-0034543860&partnerID=40&md5=de959bbf56615fddc3548fa4861e418e

Barla, A., Odone, F., & Verri, A. (n.d.). Histogram intersection kernel for image classification. In *Proceedings 2003 International Conference on Image Processing (Cat. No.03CH37429)* (Vol. 2, pp. III–513–16). IEEE. doi:10.1109/ICIP.2003.1247294

Byrd, K., Zeng, J., & Chouikha, M. (2006). An assessed digital mammography segmentation algorithm used for content-based image retrieval. In *2006 8th international Conference on Signal Processing* (Vol. 2). IEEE. doi:10.1109/ICOSP.2006.345694

Chang, H.-H., Zhuang, A. H., Valentino, D. J., & Chu, W.-C. (2009). Performance measure characterization for evaluating neuroimage segmentation algorithms. *NeuroImage*, *47*(1), 122–35. doi:10.1016/j.neuroimage.2009.03.068

Chang, R.-F., Wu, W.-J., Moon, W. K., & Chen, D.-R. (2005). Automatic ultrasound segmentation and morphology based diagnosis of solid breast tumors. *Breast Cancer Research and Treatment*, *89*(2), 179–185. Retrieved from http://www.scopus.com/inward/record.url?eid=2-s2.0-13844267711&partnerID=40&md5=e041bd7389900373ab3295633ebbfbba

Chen, D.-R., Chang, R.-F., Wu, W.-J., Moon, W. K., & Wu, W.-L. (2003). 3-D breast ultrasound segmentation using active contour model. *Ultrasound in Medicine and Biology*, *29*(7), 1017–1026. Retrieved from http://www.scopus.com/inward/record.url?eid=2-s2.0-0038104383&partnerID=40&md5=7ce9fd930964c1fa833d59c54cbee0f2

Contreras Ortiz, S. H., Chiu, T., & Fox, M. D. (2012). Ultrasound image enhancement: A review. *Biomedical Signal Processing and Control*, *7*(5), 419–428. doi:10.1016/j.bspc.2012.02.002

F. Igual R. Mayo, T. H. U. C. A. R., & M.Ujaldon. (2008). Optimizing Co-Occurrence Matrices on Graphics Processors Using Sparse Representations. In *9th Int�. Workshop on State-of-the-Art in Science and Parallel Computing, Trondheim, Norway*.

Galloway, M. M. (1975). Texture analysis using gray level run lengths. *Computer Graphics and Image Processing*, *4*(2), 172–179. doi:http://dx.doi.org/10.1016/S0146-664X(75)80008-6

Guo, Y., Cheng, H. D., Huang, J., Tian, J., Zhao, W., Sun, L., & Su, Y. (2006). Breast ultrasound image enhancement using fuzzy logic. *Ultrasound in Medicine & Biology*, *32*(2), 237–47. doi:10.1016/j.ultrasmedbio.2005.10.007

Halliwell, M. (2010). A tutorial on ultrasonic physics and imaging techniques. *Proceedings of the Institution of Mechanical Engineers, Part H: Journal of Engineering in Medicine*, *224*(2), 127–142. Retrieved from http://www.scopus.com/inward/record.url?eid=2-s2.0-76849088916&partnerID=40&md5=2e31c49ee5eacb38e9d8eff368395571

Han Chumning, Guo Huadong, & Wang Changlin. (2002). Edge preservation evaluation of digital speckle filters. In *IEEE International Geoscience and Remote Sensing Symposium* (Vol. 4, pp. 2471–2473). IEEE. doi:10.1109/IGARSS.2002.1026581

Haralick, R. M. (1979). Statistical and structural approaches to texture. *Proceedings of the IEEE*, *67*(5), 786–804. doi:10.1109/PROC.1979.11328

Huang, D.-S., McGinnity, M., Heutte, L., & Zhang, X.-P. (Eds.). (2010). *Advanced Intelligent Computing Theories and Applications* (Vol. 93). Berlin, Heidelberg: Springer Berlin Heidelberg. doi:10.1007/978-3-642-14831-6

Huang, Q.-H., Lee, S.-Y., Liu, L.-Z., Lu, M.-H., Jin, L.-W., & Li, A.-H. (2012). A robust graph-based segmentation method for breast tumors in ultrasound images. *Ultrasonics*, *52*(2), 266–275. Retrieved from http://www.scopus.com/inward/record.url?eid=2-s2.0-81855206603&partnerID=40&md5=64f63b465f4e88b93568bd6afd633289

Huang, S.-F., Chen, Y.-C., & Woo, K. M. (2008). Neural network analysis applied to tumor segmentation on 3D breast ultrasound images. In *2008 5th IEEE International Symposium on Biomedical Imaging: From Nano to Macro, Proceedings, ISBI* (pp. 1303–1306). Retrieved from http://www.scopus.com/inward/record.url?eid=2-s2.0-51049090141&partnerID=40&md5=fb1a47c542dd589d7e2fb66be1f4d161

Jiao, J., & Wang, Y. (2011). Automatic boundary detection in breast ultrasound images based on improved pulse coupled neural network and active contour model. In *5th International Conference on Bioinformatics and Biomedical Engineering, iCBBE 2011*. Retrieved from http://www.scopus.com/inward/record.url?eid=2-s2.0-79960133488&partnerID=40&md5=2fbc2be3a6c29e8afa2686a80a22de7d

Lefebvre, F., Meunier, M., Thibault, F., Laugier, P., & Berger, G. (2000). Computerized ultrasound B-scan characterization of breast nodules. *Ultrasound in Medicine & Biology*, *26*(9), 1421–1428. doi:http://dx.doi.org/10.1016/S0301-5629(00)00302-1

Legg, P. A., Rosin, P. L., Marshall, D., & Morgan, J. E. (2013). Improving accuracy and efficiency of mutual information for multi-modal retinal image registration using adaptive probability density estimation. *Computerized Medical Imaging and Graphics : The Official Journal of the Computerized Medical Imaging Society*, *37*(7-8), 597–606. doi:10.1016/j.compmedimag.2013.08.004

Liao, Y. Y., Wu, J. C., Li, C. H., & Yeh, C. K. (2011). Texture feature analysis for breast ultrasound image enhancement. *Ultrason Imaging*, *33*, 264–278.

Liu, B., Cheng, H. D., Huang, J., Tian, J., Tang, X., & Liu, J. (2010). Fully automatic and segmentation-robust classification of breast tumors based on local texture analysis of ultrasound images. *Pattern Recognition*, *43*(1), 280–298. Retrieved from http://www.scopus.com/inward/record.url?eid=2-s2.0-68949159836&partnerID=40&md5=849f4e2d8f796deb81ef01d7be063f00

Madabhushi, A., & Metaxas, D. N. (2003). Combining low-, high-level and empirical domain knowledge for automated segmentation of ultrasonic breast lesions. *IEEE Transactions on Medical Imaging*, *22*(2), 155–169. Retrieved from http://www.scopus.com/inward/record.url?eid=2-s2.0-0038398643&partnerID=40&md5=8f3c0cb69868bd81039a7d66c017a20e

Murmis, V. G., Gisvold, J. J., Kinter, T. M., & Greenleaf, J. F. (1988). Texture analysis of ultrasound B-scans to aid diagnosis of cancerous lesions in the breast. In *Ultrasonics Symposium, 1988. Proceedings., IEEE 1988* (pp. 839–842 vol.2). doi:10.1109/ULTSYM.1988.49495

Parikh, R., Mathai, A., Parikh, S., Sekhar, G. C., & Thomas, R. (2008). Understanding and using sensitivity, specificity and predictive values. *Indian Journal of Ophthalmology*, *56*(1), 45–50. Retrieved from http://www.scopus.com/inward/record.url?eid=2-s2.0-38149096396&partnerID=tZOtx3y1

Piliouras, N., Kalatzis, I., Dimitropoulos, N., & Cavouras, D. (2004). Development of the cubic least squares mapping linear-kernel support vector machine classifier for improving the characterization of breast lesions on ultrasound. *Computerized Medical Imaging and Graphics*, *28*(5), 247–255. doi:http://dx.doi.org/10.1016/j.compmedimag.2004.04.003

Rajaei, A., Dallalzadeh, E., & Rangarajan, L. (2012). Segmentation of Pre-processed Medical Images: An Approach Based on Range Filter. *International Journal of Image, Graphics and Signal Processing(IJIGSP)*, *4*(9), 8. Retrieved from http://www.mecs-press.org/ijigsp/ijigsp-v4-n9/v4n9-2.html

Rubner, Y., Tomasi, C., & Guibas, L. J. (n.d.). The Earth Mover's Distance as a Metric for Image Retrieval. *International Journal of Computer Vision*, *40*(2), 99–121. doi:10.1023/A:1026543900054

Selvarajah, S., & Kodituwakku, S. R. (2011). Analysis and Comparison of Texture Features for Content Based Image Retrieval. *International Journal of Latest Trends in Computing*, *2*(1), 108–113. Retrieved from http://www.ijltc.excelingtech.co.uk/vol2issue1/18-vol2issue1.pdf

Tang, X. (1998). Texture information in run-length matrices. *Image Processing, IEEE Transactions on*, *7*(11), 1602–1609. doi:10.1109/83.725367

Yassine, I. S., Belfkih, S., Najah, S., & Zenkouar, H. (2010). A new method for texture image segmentation. In *2010 5th International Symposium On I/V Communications and Mobile Network* (pp. 1–4). IEEE. doi:10.1109/ISVC.2010.5656161